GOCE ACCELEROMETERS DATA REVISITED: STABILITY AND DETECTOR NOISE

J. Bergé[1], B. Christophe[2], and B. Foulon[3]

[1]*ONERA, Département des Mesures Physiques, 29 avenue de la Division Leclerc, 92320 Châtillon, France. Email: joel.berge@onera.fr*

[2]*ONERA, Département des Mesures Physiques, 29 avenue de la Division Leclerc, 92320 Châtillon, France. Email: bruno.christophe@onera.fr*

[3]*ONERA, Département des Mesures Physiques, 29 avenue de la Division Leclerc, 92320 Châtillon, France. Email: bernard.foulon@onera.fr*

ABSTRACT

We report on our analyses of Gravity field and steady-state Ocean Circulation Explorer (GOCE) data aiming to characterize the stability and the noise of GOCE's accelerometers. We first measure science and detector coherence signals, which allow us to infer the role of the accelerometers Digital Voltage Amplifiers and measurement chanel in the overall quadratic factor and scale factor; we show that their temporal stability is as low as expected. We then investigate the effect of the aliasing of high frequency detector's noise on the measured noise, in an attempt to explain why the measured noise is higher than originally expected. We find that although this aliasing explains part of the higher noise, it does not account for the total of the difference seen between the expected and the measured noise.

Key words: GOCE; accelerometer; noise.

1. INTRODUCTION

The Gravity field and steady-state Ocean Circulation Explorer (GOCE) has remarkably met its goals by providing measurements of the geoid with unprecedented accuracy [4, 5]. Now that the mission is reaching its end, it is time to assess the performance of GOCE's instruments over the span of the mission.

In this work, we focus on the accelerometers at the core of GOCE's gradiometers. In particular, we aim to check their stability over time and characterize their intrinsic noise. In this sense, we define and measure good health signals which can be linked to the instrument's overall quadratic factor and scale factor.

Furthermore, although it has been known since the begining of the mission that the measured noise exceeds expectations [2, 5], it is still not understood why. Here, we investigate whether this unexpected noise level can originate from the accelerometers' detector's intrinsic noise.

This paper is organized as follow. We present GOCE's accelerometers in Section 2. Section 3 then discusses the stability the accelerometers' good health signals over time. We then discuss GOCE's accelerometers' detector noise in Section 4, before concluding in Section 5.

2. GOCE ACCELEROMETERS

GOCE gradiometers (and accelerometers) have been developed by ONERA; they are described in [3, 6]. The accelerometers are based on control loops so that the proof-mass stays at the center of its electrodes cage. The same control loops also control the drag free system. Science data are obtained after filtering along the science chanel, diverted from the control loop. External accelerations are therefore measured as the (scaled) voltages, sent to the electrodes by the control loop, that are required to keep the proof mass at the center of its cage.

Figure 1 shows how each accelerometer's electronics control loop works. The motion of the proof-mass (gray square) in its cage is detected as an analogic voltage by a capacitive detector and converted into a 1027.96 Hz digital signal by the Analogic-to-Digital-Converter ADC1 (yellow). This signal is used by a proportional-integral-derivative (PID) controller (pink) whose output is both diverted to the drag free system (DFACS) and reinjected in the loop, where it is converted back to an analogic signal (blue) before being fed back to the proof-mass' cage's electrodes.

At this point, the analogic signal is also diverted to the science branch: it is first read, converted into a digital signal and downsampled to 10.2796 Hz (Readout and ADC2 – green). It then goes through the science filter, at which point it is downsampled at 1 Hz, before being stored for its eventual science analysis.

The signal can be measured at different points in the loop. This allows us to check on the various systems of the loop and assess the instrument's good health. For instance, detector output's voltages are continuously stored as 1/8

Proc. 'ESA Living Planet Symposium 2013', Edinburgh, UK
9–13 September 2013 (ESA SP-722, December 2013)

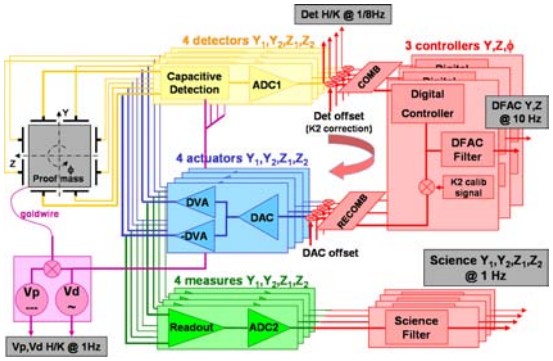

Figure 1. Accelerometer control loop. The motion of the proof mass in its electrodes cage (gray) is sensed by a capacitive detector (yellow) and controlled by a digital controller (pink). The same loop controls the satellite's drag-free system. Science data are obtained after filtering along the science chanel (lower part of the sketch).

Hz house-keeping data. In the next section, we define two good health signals, whose stability over time we assess and compare with that of the instrument's quadratic factor and scale factor.

3. DETECTOR AND SCIENCE BRANCH STABILITY

In this section, we aim to characterize the long term stability of the accelerometers subsystems through the evolution of good health signals. Those signals provide a handle on the role of the detector and of the measurement chanel in the evolution of the quadratic factor K2 and scale factor $k_{\rm Sci}$.

3.1. Detector coherence

The detector coherence along the Y and Z (ultrasensitive) axes is defined as

$$GHDET_{YZ} = -V_{Y1} + V_{Y2} - V_{Z1} + V_{Z2} \qquad (1)$$

where the voltages $V_{\kappa i}$ are taken at the detector's output. It can be shown that this coherence signal appears in the first-order approximation of the instrument's quadratic factor through a bias y_0 to which it is directly linked:

$$K2 = \frac{1}{V_p G_{el}} \left(\frac{dG_{Ad}}{G_A} - \frac{y_0}{e} \right) \qquad (2)$$

where V_p is the polarization voltage, G_{el} is the electrostatic gain, G_A is the Digital Voltage Amplifiers (DVA)'s gain and e is the gap between the proof mass and the electrodes.

Thus, the time evolution of the detector's good health provides us with a proxy on the effect of the DVA on the quadratic factor's evolution. Figure 2 shows the evolution of $GHDET_{YZ}$ for all six accelerometers from November 2009 to August 2011. A linear fit to each curve provides a value for the drift of accelerometers' $GHDET_{YZ}$: we find that the drift is similar for all accelerometers, with the biggest for accelerometers 2 and 4, of 1.45×10^{-5} V/day. Using the aforementioned link to the quadratic factor, we can infer that the drift caused by the DVA on the quadratic factor does not exceed 0.11 s^2/m/month. This is well below the specification of 1 s^2/m/month.

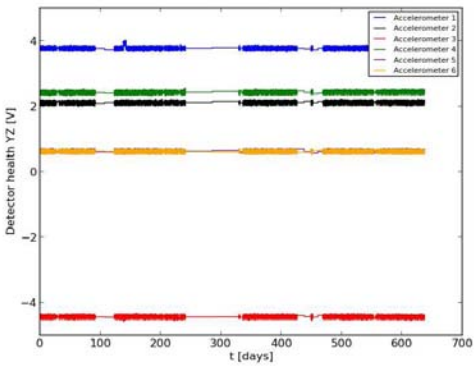

Figure 2. Time evolution, from November 2009 to August 2011, of the detector's good health signal for each accelerometer.

3.2. Science coherence

The science coherence along the Z axis is defined as

$$V_{\rm SciCohZ} = \frac{V_{\rm SciZ1} - V_{\rm SciZ2}}{2} \qquad (3)$$

and can be shown to be linked to the science output $V_{\rm SciZ} = (V_{\rm SciZ1} + V_{\rm SciZ2})/2$ through, at first order,

$$V_{\rm SciCohZ} = \left(\frac{dG_m}{G_m} + \frac{dG_A}{G_A} \right) V_{\rm SciZ} + \text{constant} \qquad (4)$$

where G_m is the measurement gain. Moreover, it can be shown that at first order, the scale factor depends on dG_m/G_m as $k_{\rm Sci} = 1 + dG_m/G_m$. Hence, estimating the correlation between the science coherence and the science outputs gives a clue about the role of the measurement gain and of the DVA gain in the scale factor evolution over time.

Figure 3 shows the evolution of the science coherence (upper panel) and of the science output (lower panel) over a 2-day period, for accelerometer 2. A correlation is clearly visible, whose evolution over time can be assessed by computing it at different dates. Figure 4 shows this information for all six accelerometers. It shows the correlation between the science coherence and the science output computed for individual days over the period

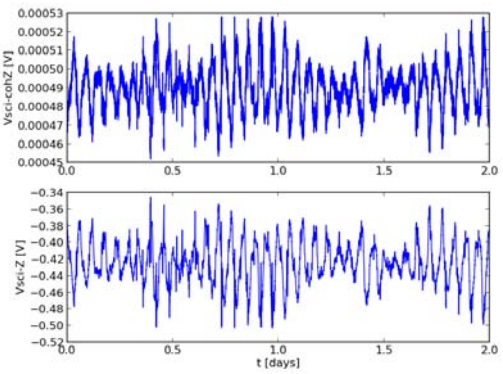

Figure 3. Time evolution, over a 2-day period, of the science coherence (upper panel) and of the science output (lower panel) for accelerometer 2.

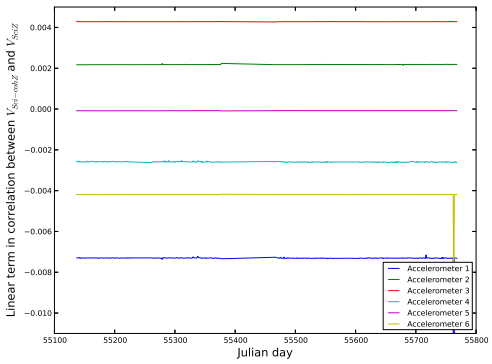

Figure 4. Evolution of the correlation between the science coherence and the science output, from November 2009 to August 2011 for all six accelerometers. Symbols show the correlation for individual days.

from November 2009 to August 2011. A linear trend is visible for each accelerometer, which we fit with a second order polynomial. This provides us with the drifts on the scale factor induced by the measurement and DVA gains: they do not exceed 10^{-6} month^{-1}. These drifts shall be compared with the measured overall scale factor drifts, estimated about a few 10^{-5} month^{-1}. Therefore, the combination of the measurement and DVA gains does not explain the measured drift of the scale factor.

4. DETECTOR NOISE

The ADC1 (yellow box in Fig. 1) is characterized by a non-trivial noise whose spectral density shows a fast f^2 increase at high frequency. As a consequence, it tends to dominate over other sources of noise in the accelerometers' control loop. In this section, we aim to (1) check whether the ADC1s on-board GOCE behave as expected, and to (2) propagate the effect of this colored noise to the

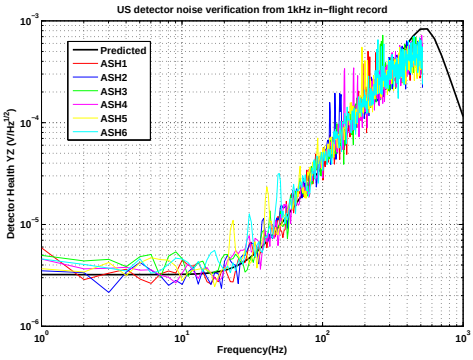

Figure 5. ADC1 good health signal's spectral density. Black line: expected signal. Colored lines: measured signal for each accelerometer.

science output. Our goal is to check whether this could be the source of the discrepancy between the expected noise and the measured one.

4.1. Detector noise behavior

We first use 1 kHz recordings of the signal output from the detector to check on the ADC1 noise. Fig. 5 shows our results, presented as the spectral density (SD) of the corresponding good health signal. The black curve shows the expected SD, which increases up to $f = 500$ Hz, where it is cut by the ADC cut-off. The colored curves show the measured SD for each accelerometer. They all agree remarkably well with the expectation. Therefore, all ADC1s behave as expected on-board GOCE.

4.2. Aliasing from high frequency noise

We now aim to investigate the effect of the ADC1 noise on the external acceleration measurement. As aforementioned, the ADC1 noise increases at high frequencies. The analyses performed during the instrument's development assumed that this would not impact the total noise in the measurement bandwidth, and calculations were done by modeling the ADC1 noise by a white noise.

To investigate whether the ADC1 colored noise can account for the unexpected noise level, we developed a numerical simulation of a GOCE accelerometer. In order to minimize the contamination to the response to the noise, our simulations ignore the coupling between different axes of the accelerometer, and we focus only on one axis (this paper shows results for the Z axis). Furthermore, to speed up the simulation, we simulate only one ADC1, instead of two (each accelerometer has two ADC1s). To be coherent with reality, the noise level of the ADC1 considered in the simulation is the real one divided by $\sqrt{2}$.

We are mostly interested in how the high-frequency noise

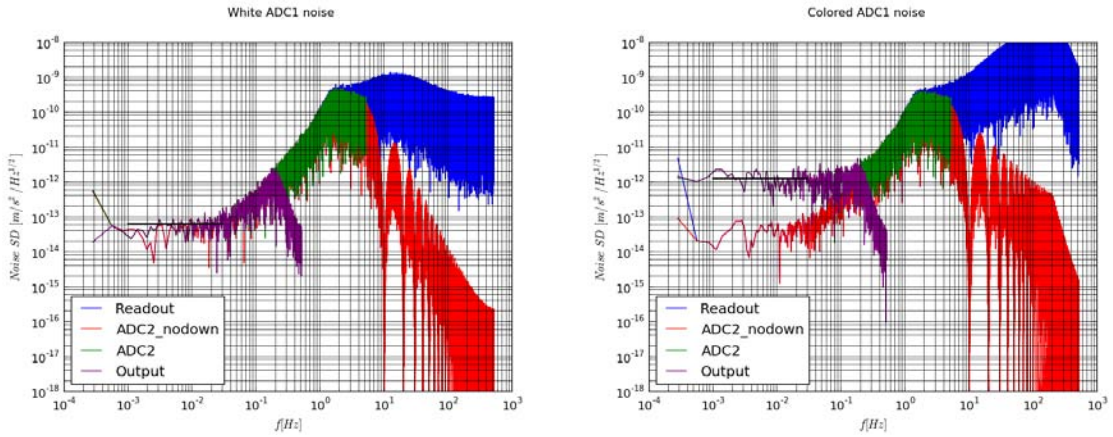

Figure 6. Instrument's noise spectral density at different stages of the science branch: readout (blue), ADC2 before downsampling from 1027.96 Hz to 10.2796 Hz (red), ADC2 after downsampling (green) and science output (purple), when the ADC1 noise is assumed white (left panel) or colored (right panel). Note that the y-axis scales are the same in both panels.

from ADC1 is propagated through the control loop and through the science branch. For the sake of simplicity, we simulate the output ADC1 as a time series with spectral density (SD) as described above (Fig. 5).

To assess the response to the ADC1 noise, we simulate the output of a null external signal, i.e. the only signal in the accelerometer is the ADC1 noise. We compare both cases where (1) the ADC1 noise is white (i.e. the f^2 increase at high frequencies is ignored) and (2) where the frequency-dependence of the ADC1 is taken into account.

The left panel of Fig. 6 shows the spectral density of the signal, when assuming a white ADC1 noise, at different points in the science branch: after the readout (blue), after the ADC2 (before –red– and after –green– downsampling) and at the output of the branch (purple). All signals are scaled as accelerations (i.e., such that their SDs are expressed in m/s^2/Hz$^{1/2}$). The right panel of the figure shows the same information, when the ADC1's noise depends on frequency. This figure shows that the increase of ADC1 at high frequencies results in a noise whose SD drops significantly slower at high frequency, even after being filtered by the ADC2. This in turn results in a significant aliasing during downsampling from 1027.96 Hz to 10.2796 Hz, and in a significantly higher noise SD in the measurement frequency band. We checked that the decimation from 10.2796 Hz to 1.02796 Hz after the science filter does not affect the noise level.

The aliasing of high frequencies is significant during the downsampling from 1027.96 Hz to 10.2796 Hz in the science branch. It results in the noise level coming from the ADC1 being an order of magnitude higher than previously estimated when assuming that this noise was white. The impact on the overall noise is showed in Figure 7, which shows the different noise sources contributions when the ADC1 is assumed white (left panel) or colored (right panel). In each panel, the red curve shows the total noise, which is to be compared with the requirements (black curve). Other curves show the noise from individual sources; the ADC1 noise is represented by the solid purple line. Although its aforementioned order-of-magnitude increase is well visible, it is so small that its effect in the total noise is limited. We can nonetheless see a small increase of the total noise, which now exceeds the requirements, with a level in the measurement bandwidth around 2.3×10^{-12} m/s^2/Hz$^{1/2}$. This level is higher than expected, yet it does not completely explain the increase of the gravity gradient tensor (GGT) noise (from GGT measurement, the accelerometer noise of pair 1-4 is 3.9×10^{-12} m/s^2/Hz$^{1/2}$, the noise of pair 2-5 is 3.1×10^{-12} m/s^2/Hz$^{1/2}$ and the noise of pair 3-6 is 6.7×10^{-12} m/s^2/Hz$^{1/2}$ [5, 1]).

5. CONCLUSION

We used GOCE data to analyze long term variations of the accelerometers' detector and science good health signals. Those signals should remain nearly constant over the mission span. We indeed found that their drifts are significantly lower than those set by the mission requirements. By relating those signals to the instrument's quadratic factor and scale factor, we showed that the contribution of the accelerometers' DVA and measurement chanel in those factors is negligible.

We then investigated the contribution of the accelerometers' ADC1 noise in the total science output noise. After checking that the ADC1s behave as expected, we used numerical simulations to show that the aliasing of high frequency noise coming from the ADC1s causes an increase of the total noise level in the measurement bandwidth. This aliasing had not been noticed before since the models used incorrectly assumed that the ADC1 noise was white. Yet, the increase in the noise due to this aliasing is not enough to explain the discrepancy between the

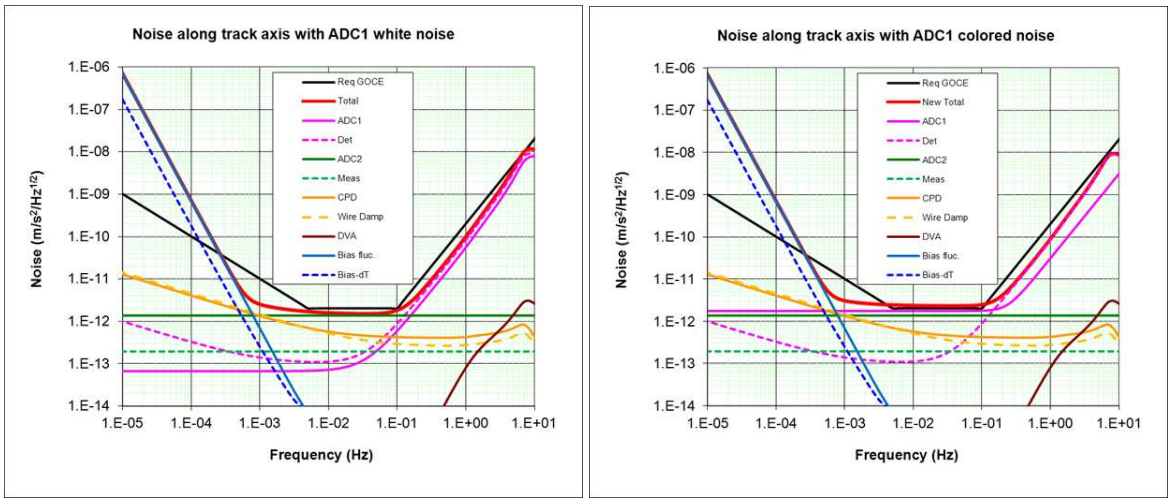

Figure 7. Noise spectral density when the ADC1 noise is assumed white (left panel) or colored (right panel).The total noise appears in red, and should be compared with the requirements (black lines). The ADC1 noise is shown by the solid purple line. Note that the y-axis scales are the same in both panels.

expected noise and the measured one. Hence, we will explore other possible sources of noise, such as non-linearities in the control loop. Furthermore, our work does not explain why this discrepancy depends on the axis. Therefore, we plan to analyze how this increase of noise could depend on the level of the acceleration, explaining the difference of noise for the different axes.

Although this work emphasizes the role of an imperfect filtering of the signal, we should note that due to constraints in the design of the GOCE accelerometers, it was not possible to apply a better filter to the high frequency noise in order to avoid its aliasing. Since this problem stems from the use of a hybrid analogic – digital instrument, we can think of improvements for future gravity missions; for instance, the Grace Follow-On accelerometers are entirely analogic, and hence should not suffer the same problem.

ACKNOWLEDGMENTS

The authors wish to thank Thales Alenia Space and ESA for providing them with GOCE data.

REFERENCES

[1] B. Christophe et al, In-flight verification of the GOCE accelerometers, in prep

[2] J-P. Marque, B. Christophe, B. Foulon, 2010, Accelerometers of the GOCE mission: return of experience from one year of in-orbit data, Living Planet Symposium 2010

[3] J-P. Marque, B. Christophe, B. Foulon, 2010, In-orbit data of the accelerometers of the ESA GOCE mission, 61st IAC Congress, Prague, CZ, IAC-10.B1.3.1

[4] R. Pail, S. Bruinsma, F. Migliaccio et al., 2011, First GOCE gravity field models derived by three different approaches, Journal of Geodesy, 85, 819

[5] R. Rummel, W. Yi, C. Stummer, 2011, GOCE gravitational gradiometry, Journal of Geodesy, 85, 777

[6] P. Touboul, B. Foulon, J-P. Marque, B. Christophe, 2009, CHAMP, GRACE, GOCE instruments and beyond, Geodesy for Planet Earth, IAG Assembly, Buenos Aires, Argentina, Springer Heidelberg Dordrecht London New York, Library of Congress Control Number 2011941192